

See discussions, stats, and author profiles for this publication at: <https://www.researchgate.net/publication/253043139>

# HfO<sub>2</sub> and Al<sub>2</sub>O<sub>3</sub> gate dielectrics on GaAs grown by atomic layer deposition

Article in Applied Physics Letters · April 2005

DOI: 10.1063/1.1899745

CITATIONS

323

READS

295

8 authors, including:



Martin M. Frank

IBM

126 PUBLICATIONS 4,733 CITATIONS

[SEE PROFILE](#)



Dmitri Starodub

Stanford University

53 PUBLICATIONS 5,144 CITATIONS

[SEE PROFILE](#)



Torgny Gustafsson

Rutgers, The State University of New Jersey

225 PUBLICATIONS 8,454 CITATIONS

[SEE PROFILE](#)

Some of the authors of this publication are also working on these related projects:



functionalization [View project](#)



SIMS analysis of high-k metal gate stacks [View project](#)

# HfO<sub>2</sub> and Al<sub>2</sub>O<sub>3</sub> gate dielectrics on GaAs grown by atomic layer deposition

Martin M. Frank<sup>a)</sup>

IBM Semiconductor Research and Development Center (SRDC), Thomas J. Watson Research Center, Yorktown Heights, New York 10598

Glen D. Wilk

ASM America, Phoenix, Arizona 85034

Dmitri Starodub, Torgny Gustafsson, Eric Garfunkel, and Yves J. Chabal

Rutgers University, Departments of Physics and Chemistry, and Laboratory for Surface Modification, Piscataway, New Jersey 08854

John Grazul and David A. Muller

Cornell University, Center for Materials Research, Ithaca, New York 14853

(Received 13 January 2005; accepted 26 February 2005; published online 4 April 2005)

High-performance metal-oxide-semiconductor field effect transistors (MOSFETs) on III–V semiconductors have long proven elusive. High-permittivity (high- $\kappa$ ) gate dielectrics may enable their fabrication. We have studied hafnium oxide and aluminum oxide grown on gallium arsenide by atomic layer deposition. As-deposited films are continuous and predominantly amorphous. A native oxide remains intact underneath HfO<sub>2</sub> during growth, while thinning occurs during Al<sub>2</sub>O<sub>3</sub> deposition. Hydrofluoric acid etching prior to growth minimizes the final interlayer thickness. Thermal treatments at  $\sim 600$  °C decompose arsenic oxides and remove interfacial oxygen. These observations explain the improved electrical quality and increased gate stack capacitance after thermal treatments. © 2005 American Institute of Physics. [DOI: 10.1063/1.1899745]

Metal-oxide-semiconductor field-effect transistors (MOSFETs) on III–V semiconductor would offer a number of advantages over Si-based devices. The higher carrier mobility would lead to faster complementary MOS (CMOS) logic operation, higher breakdown fields would support high-power/temperature applications, band structure engineering would offer design flexibility, and monolithic optoelectronic circuits would likely become manufacturable.

However, MOSFETs on high-carrier-mobility substrates (compound semiconductors as well as germanium) have been elusive due to the lack of high-quality gate insulators, mostly because of the absence of stable passivating native oxides and the high density of slow interface traps ( $D_{it}$ ) with deposited oxides.<sup>1</sup> For example, Fermi level pinning upon GaAs oxidation has been attributed to oxygen-induced displacement of surface As atoms, where doubly O-coordinated second-layer Ga atoms give rise to gap states.<sup>2</sup> Excess interfacial As occupying As<sub>Ga</sub> antisite defects causes gap states as well.<sup>2,3</sup> Such As may be formed via decomposition of As<sub>2</sub>O<sub>3</sub> in the vicinity of GaAs, resulting from the reaction: As<sub>2</sub>O<sub>3</sub> + 2GaAs → Ga<sub>2</sub>O<sub>3</sub> + 4As.<sup>4</sup> Until recently, oxide/III–V interfaces with low  $D_{it}$  had to be fabricated by molecular beam epitaxy (MBE) of Ga<sub>2</sub>O<sub>3</sub> (where Gd was added to reduce leakage)<sup>1,5</sup> or Al<sub>2</sub>O<sub>3</sub>.<sup>6</sup> Fermi level unpinning in the Ga<sub>2</sub>O<sub>3</sub>/GaAs system has been attributed to a Ga<sub>2</sub>O/GaAs-like interface in which the Ga and As surface atoms are restored to near-bulk charge.<sup>2</sup>

Atomic layer deposition (ALD) or chemical vapor deposition (CVD) is technologically more attractive than MBE. The recent development of high-quality ALD- and CVD-grown high-permittivity (high- $\kappa$ ) gate dielectrics on Si justifies some optimism regarding integration on III–V

substrates.<sup>7</sup> Gate stacks for depletion mode MOSFETs with  $D_{it} < 10^{12}$  cm<sup>-2</sup> eV<sup>-1</sup> were recently fabricated by ALD of Al<sub>2</sub>O<sub>3</sub> onto native oxide covered GaAs.<sup>8–10</sup> A 600–650 °C anneal in O<sub>2</sub> minimized current–voltage hysteresis and frequency dispersion, and maximized gate stack capacitance. Transmission electron microscopy (TEM) pointed to a remarkably sharp Al<sub>2</sub>O<sub>3</sub>/GaAs interface, prompting the speculation that the native oxide is removed during the ALD process. ALD-grown Al<sub>2</sub>O<sub>3</sub> also results in good gate stack properties on InGaAs<sup>11</sup> and AlGaIn/GaN<sup>12</sup> and may be used to coat compound semiconductor nanowires conformally.<sup>13</sup> By contrast, very few studies have been published regarding the most important high- $\kappa$  gate dielectric, HfO<sub>2</sub>, on III–V semiconductors.<sup>14,15</sup>

In this letter, we characterize the structure and composition of Al<sub>2</sub>O<sub>3</sub>/GaAs and HfO<sub>2</sub>/GaAs, to help develop an understanding of the impact of material and processing conditions on the quality of ALD-grown high- $\kappa$ /III–V stacks. We address successive stages of stack formation: starting surface, temperature ramp-up, ALD process, and anneal. Both Al<sub>2</sub>O<sub>3</sub> and HfO<sub>2</sub> were grown on oxide-covered (epiready) and HF-etched GaAs(100). For high- $\kappa$  dielectric growth, we followed a procedure that recently yielded high-quality Al<sub>2</sub>O<sub>3</sub>/GaAs gate stacks.<sup>8–10</sup> Depositions were performed using alternating exposures of the common ALD precursors Al(CH<sub>3</sub>)<sub>3</sub>+H<sub>2</sub>O or HfCl<sub>4</sub>+H<sub>2</sub>O in a N<sub>2</sub> carrier gas at 300 °C, using a commercial ASM Pulsar3000™ ALD reactor. C or Al served as caps for microscopy. Films were characterized *ex situ* by scanning TEM (STEM), electron energy loss spectroscopy (EELS), transmission infrared spectroscopy (70° off-normal), medium energy ion scattering (MEIS), and x-ray photoelectron spectroscopy (XPS).

The epiready oxide on GaAs was found by STEM to have a thickness of 20–25 Å [Fig. 1(a)]. The layer is Ga-rich

<sup>a)</sup>Electronic mail: mmfrank@us.ibm.com

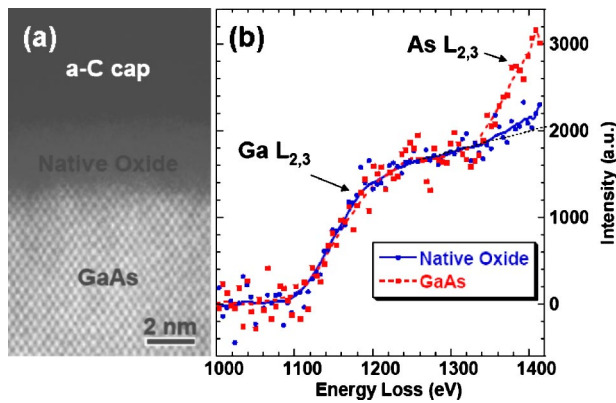


FIG. 1. (Color online) (a) STEM image and (b) STEM-EELS spectra in the Ga and As  $L_{2,3}$  regions from C-capped epitaxial oxide on GaAs(100). Spectra were recorded within the native oxide and in the GaAs substrate.

(As:Ga=0.17), as determined by STEM-EELS [Fig. 1(b)], with an increased As concentration near the GaAs substrate. Areal densities of O and (Ga+As) in the oxide are  $3.2$  and  $3.3 \times 10^{15} \text{ cm}^{-2}$ , respectively, as measured by MEIS, consistent with a porous (50% of bulk density) mixture of known oxides containing a high fraction of  $\text{Ga}_2\text{O}_3$ . In the following, we will denote this substrate Ga(As)O/GaAs. HF-etched substrates, on the other hand, are mostly oxide-free.<sup>16</sup>

During a vacuum preanneal of Ga(As)O/GaAs to the ALD temperature of  $300^\circ\text{C}$ , there is only a 7% reduction in O content, while most surface hydrocarbons desorb (as measured by MEIS, not shown). The lack of any substantial thinning of Ga(As)O during inert anneal to  $300^\circ\text{C}$  is consistent with the higher onset temperatures of reactions in, e.g., thermal ( $300\text{--}390^\circ\text{C}$ ),<sup>17</sup> anodic ( $430^\circ\text{C}$ ),<sup>4</sup> and wet-chemical/native ( $320^\circ\text{C}$ )<sup>18</sup> oxides on GaAs.

The as-deposited high- $\kappa$  films are continuous, i.e., not islanded, and appear amorphous in TEM images (Fig. 2). Infrared spectroscopy confirms that  $\text{Al}_2\text{O}_3$  films on Ga(As)O/GaAs are amorphous, as for ALD-grown  $\text{Al}_2\text{O}_3$  on Si.<sup>19</sup> This is evidenced by absorption features at  $720$  and  $955 \text{ cm}^{-1}$  [Fig. 3(a)] which may be assigned to transverse-optical (TO) and longitudinal-optical (LO) phonon modes of amorphous  $\text{Al}_2\text{O}_3$ , respectively. In contrast, for  $\text{HfO}_2$  a signal at  $700 \text{ cm}^{-1}$  and its high-frequency shoulder [Fig. 3(b)] may

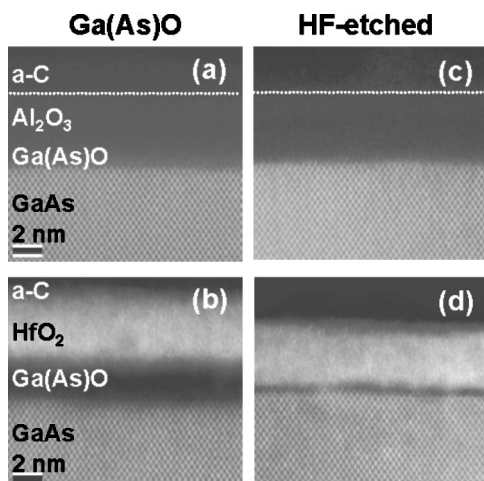


FIG. 2. STEM images from  $40 \text{ \AA}$   $\text{Al}_2\text{O}_3$  (top) and  $\text{HfO}_2$  (bottom) deposited onto Ga(As)O-covered [(a) and (b)] and HF-etched [(c) and (d)] GaAs(100).

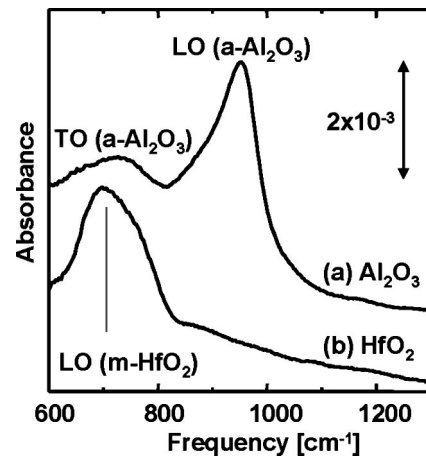


FIG. 3. Transmission infrared spectra from (a)  $40 \text{ \AA}$   $\text{Al}_2\text{O}_3$  and (b)  $40 \text{ \AA}$   $\text{HfO}_2$  deposited onto Ga(As)O/GaAs(100). “a” and “m” denote amorphous and monoclinic oxides, respectively.

be attributed to monoclinic  $\text{HfO}_2$ ,<sup>20</sup> indicating crystalline inclusions in an amorphous matrix.

The structure and composition of the high- $\kappa$ /GaAs stack depends on the nature of the starting surface. At a target high- $\kappa$  thickness of  $40 \text{ \AA}$ , the areal densities of metal ions are slightly higher on HF-etched substrates than on oxide-covered substrates (by 14% for  $\text{Al}_2\text{O}_3$  and by 6% for  $\text{HfO}_2$ ; MEIS, not shown). This may indicate high- $\kappa$  agglomeration during initial growth on HF-etched GaAs, similar to what has been observed for HF-etched Ge.<sup>21</sup>

Interfacial layer thicknesses after  $\text{Al}_2\text{O}_3$  and  $\text{HfO}_2$  deposition onto Ga(As)O/GaAs are  $\sim 10$  and  $20\text{--}25 \text{ \AA}$ , respectively [Figs. 2(a) and 2(b)]. When native oxide removal by an initial HF wet etch is performed instead, both  $\text{Al}_2\text{O}_3$  and  $\text{HfO}_2$  deposition result in low interfacial layer thicknesses of only  $3\text{--}8 \text{ \AA}$  [Figs. 2(c) and 2(d)]. MEIS data support this finding, indicating near-stoichiometric O:Al and O:Hf ratios of 1.51 and 2.04, respectively, for etched substrates, as opposed to oxygen-rich ratios of 1.70 and 2.33 for oxide-covered substrates, with excess oxygen attributed to interfacial Ga(As)O.

The TEM observation of only  $\sim 10 \text{ \AA}$  interfacial oxide for  $\text{Al}_2\text{O}_3$ /Ga(As)O/GaAs indicates that the initial oxide is thinned during the  $\text{Al}_2\text{O}_3$  ALD growth process. This points to volatilization of Ga(As)O or its conversion into  $\text{Al}_2\text{O}_3$ . By contrast, the  $\text{HfO}_2$  growth process does not cause interface thinning, even though the standard Gibbs energies of formation per O atom are nearly identical ( $\text{Al}_2\text{O}_3$ :  $-527 \text{ kJ/mol}$ ;  $\text{HfO}_2$ :  $-544 \text{ kJ/mol}$ ) and both higher than for Ga and As oxides.<sup>4,22</sup> The different degree of interface thinning likely is due to the much higher reactivity of  $\text{Al}(\text{CH}_3)_3$  compared to  $\text{HfCl}_4$ , reflected in standard enthalpies of formation of  $-74 \text{ kJ/mol}$  and  $-990 \text{ kJ/mol}$ , respectively.<sup>22,23</sup> Also, ALD reaction with hydroxylated oxides has been shown to be much more favorable for  $\text{Al}(\text{CH}_3)_3$  than for  $\text{HfCl}_4$ .<sup>24–26</sup>

The residual interfacial oxide remains Ga-rich during ALD growth, as shown by STEM-EELS, with As oxides still present in the case of  $\text{Al}_2\text{O}_3$  on Ga(As)O/GaAs (XPS data in Fig. 4; As oxide signal at  $44.8 \text{ eV}$ ).<sup>27</sup> For all interfaces, TEM images indicate disorder or random strain in the topmost 1–2 GaAs unit cells. The presence of amorphous interfacial GaAs is confirmed by excess visible GaAs in MEIS.

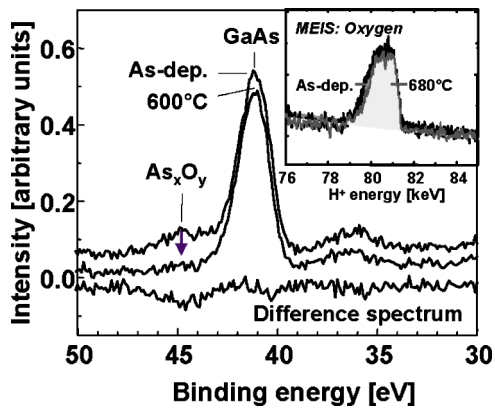


FIG. 4. XPS spectra in the As  $3d$  region from  $40 \text{ \AA}$   $\text{Al}_2\text{O}_3$  deposited onto Ga(As)O/GaAs(100) before (top) and after (center) vacuum anneal to  $600 \text{ }^\circ\text{C}$ , and difference spectrum (bottom). Inset: MEIS spectra in the oxygen region before and after vacuum anneal to  $680 \text{ }^\circ\text{C}$ .

During vacuum anneals of  $\text{Al}_2\text{O}_3$  on Ga(As)O/GaAs at  $600\text{--}680 \text{ }^\circ\text{C}$ , the As oxides decompose, as detected by changes in the XPS spectrum (Fig. 4).<sup>27</sup> Indeed, most oxygen is removed from the interfacial layer (decrease of  $2.5 \times 10^{15} \text{ O cm}^{-2}$  for a  $40 \text{ \AA}$   $\text{Al}_2\text{O}_3$  film), as evidenced by an intensity drop on the low ion energy side of the MEIS oxygen peak (Fig. 4, inset). This thermal behavior may be rationalized by recalling results for oxidized GaAs surfaces (without a high- $\kappa$  layer) in inert ambients.<sup>4,17,18,28,29</sup> At  $300\text{--}460 \text{ }^\circ\text{C}$ , mixed gallium/arsenic oxides are converted into pure gallium oxide with As precipitates according to the reaction  $\text{As}_2\text{O}_3 + 2\text{GaAs} \rightarrow \text{Ga}_2\text{O}_3 + 4\text{As}$  (with partial As desorption in the form of  $\text{As}_2$  and  $\text{As}_4$ ). At  $\sim 475 \text{ }^\circ\text{C}$ , any  $\text{Ga}_2\text{O}_3$  present in the film desorbs; and at  $580\text{--}630 \text{ }^\circ\text{C}$ , the remaining  $\text{Ga}_2\text{O}_3$  is volatilized according to  $\text{Ga}_2\text{O}_3 + 4\text{GaAs} \rightarrow 3\text{Ga}_2\text{O} \uparrow + 4\text{As} \uparrow$ . At similar temperatures, preferential As desorption from the GaAs substrate sets in. Assuming analogous reactions underneath the high- $\kappa$  layers, including facile outdiffusion of volatile species, a  $\sim 600 \text{ }^\circ\text{C}$  anneal would thus result in (a) a  $\text{Ga}_2\text{O}_3$ -like interfacial layer which, upon continued heating, may be partially or completely removed, and (b) excess interfacial Ga. While we presently do not have any direct experimental evidence for the presence of  $\text{Ga}_2\text{O}_3$ , our findings of As oxide decomposition and oxygen loss are consistent with this reaction scheme.

The role of the  $\text{O}_2$  ambient during the  $600\text{--}650 \text{ }^\circ\text{C}$  anneal employed in the device studies of ALD-grown  $\text{Al}_2\text{O}_3/\text{GaAs}$  stacks<sup>8–10</sup> remains to be explained. Electrical measurements indicate that no additional interfacial oxide grows in  $\text{O}_2$ .<sup>30</sup> Therefore, the primary difference between mildly oxidizing and reducing anneals may be the oxidation and desorption of excess interfacial Ga.  $\text{O}_2$  In addition, may improve high- $\kappa$  quality, volatilizing As or Ga diffused into the layer and filling detrimental oxygen vacancies.

In conclusion, the interfacial layer thickness and composition in ALD-grown high- $\kappa/\text{GaAs}$  stacks, and thus the device properties, are determined by surface preparation, growth chemistry, and thermal treatments. GaAs oxide remains in place during  $\text{HfO}_2$  growth, while partial removal or conversion of the oxide to  $\text{Al}_2\text{O}_3$  occurs during the  $\text{Al}_2\text{O}_3$  ALD process. HF etching prior to growth leads to stacks with reduced interfacial layer thickness. Thermal treatments at  $\sim 600 \text{ }^\circ\text{C}$  decompose interfacial As oxides and remove

oxygen. This may explain the improved electrical quality and increased capacitance of such structures.

Film growth as well as STEM and infrared analysis were performed at and supported by Bell Laboratories MEIS was performed at Rutgers University and supported by NSF and SRC. M.M.F. was supported by a fellowship from DAAD. D.R.M. and J.G. were supported by the NSF through Cornell's MRSEC Program

<sup>1</sup>M. Hong, C. T. Liu, H. Reese, and J. Kwo, in *Wiley Encyclopedia of Electrical and Electronics Engineering*, edited by J. G. Webster (Wiley, New York, 1999), Vol. 19, p. 87.

<sup>2</sup>M. J. Hale, S. I. Yi, J. Z. Sexton, A. C. Kummel, and M. Passlack, *J. Chem. Phys.* **119**, 6719 (2003).

<sup>3</sup>W. E. Spicer, Z. Liliental-Weber, E. Weber, N. Newman, T. Kendelewicz, R. Cao, C. McCants, P. Mahowald, K. Miyano, and I. Lindau, *J. Vac. Sci. Technol. B* **6**, 1245 (1988).

<sup>4</sup>K. Eguchi and T. Katoda, *Jpn. J. Appl. Phys., Part 1* **24**, 1043 (1985).

<sup>5</sup>M. Passlack, N. Medendorp, S. Zollner, R. Gregory, and D. Braddock, *Appl. Phys. Lett.* **84**, 2521 (2004).

<sup>6</sup>J. S. Hwang, C. C. Chang, M. F. Chen, C. C. Chen, K. I. Lin, F. C. Tang, M. Hong, and J. Kwo, *J. Appl. Phys.* **94**, 348 (2003).

<sup>7</sup>G. D. Wilk, R. M. Wallace, and J. M. Anthony, *J. Appl. Phys.* **89**, 5243 (2001).

<sup>8</sup>P. D. Ye, G. D. Wilk, J. Kwo, B. Yang, H.-J. L. Gossmann, M. Frei, S. N. G. Chu, J. P. Mannaerts, M. Sergent, M. Hong, K. K. Ng, and J. Bude, *IEEE Electron Device Lett.* **24**, 209 (2003).

<sup>9</sup>P. D. Ye, G. D. Wilk, B. Yang, J. Kwo, S. N. G. Chu, S. Nakahara, H.-J. L. Gossmann, J. P. Mannaerts, M. Hong, K. K. Ng, and J. Bude, *Appl. Phys. Lett.* **83**, 180 (2003).

<sup>10</sup>P. D. Ye, G. D. Wilk, B. Yang, J. Kwo, H. J. L. Gossmann, M. Frei, J. P. Mannaerts, M. Sergent, M. Hong, K. K. Ng, and J. Bude, *J. Electron. Mater.* **33**, 912 (2004).

<sup>11</sup>P. D. Ye, G. D. Wilk, B. Yang, J. Kwo, H. J. L. Gossmann, M. Hong, K. K. Ng, and J. Bude, *Appl. Phys. Lett.* **84**, 434 (2004).

<sup>12</sup>P. D. Ye, B. Yang, K. K. Ng, J. Bude, G. D. Wilk, S. Halder, and J. C. M. Hwang, *Appl. Phys. Lett.* **86**, 063501 (2005).

<sup>13</sup>B. Min, J. S. Lee, K. Cho, J. W. Hwang, H. Kim, M. Y. Sung, S. Kim, J. Park, H. W. Seo, S. Y. Bae, M.-S. Lee, S. O. Park, and J.-T. Moon, *J. Electron. Mater.* **32**, 1344 (2003).

<sup>14</sup>M. Kusaka, M. Hirai, and S. Okazaki, *Rep. R. L. Surf. Sci., Okayama U.* **4**, 245 (1978).

<sup>15</sup>M. Fanciulli, S. Spiga, G. Scarel, G. Tallarida, C. Wiemer, and G. Seguini, *Mater. Res. Soc. Symp. Proc.* **786**, E6.14.1 (2004).

<sup>16</sup>S. Adachi and D. Kikuchi, *J. Electrochem. Soc.* **147**, 4618 (2000).

<sup>17</sup>K. Tone, M. Yamada, Y. Ide, and Y. Katayama, *Jpn. J. Appl. Phys., Part 2* **31**, L721 (1992).

<sup>18</sup>F. Schröder, W. Storm, M. Altebockwinkel, L. Wiedmann, and A. Bennighoven, *J. Vac. Sci. Technol. B* **10**, 1291 (1992).

<sup>19</sup>M. M. Frank, Y. J. Chabal, and G. D. Wilk, *Appl. Phys. Lett.* **82**, 4758 (2003).

<sup>20</sup>M. M. Frank, S. Sayan, S. Dörmann, T. J. Emge, L. S. Wielunski, E. Garfunkel, and Y. J. Chabal, *Mater. Sci. Eng., B* **109**, 6 (2004).

<sup>21</sup>A. Delabie, R. L. Puurunen, B. Brijs, M. Caymax, T. Conard, B. Onsia, O. Richard, W. Vandervorst, C. Zhao, M. M. Heyns, M. Meuris, M. M. Vii-tanen, H. H. Brongersma, M. de Ridder, L. V. Goncharova, E. Garfunkel, T. Gustafsson, and W. Tsai, *J. Appl. Phys.* **97**, 064104 (2005).

<sup>22</sup>D. R. Lide, *CRC Handbook of Chemistry and Physics*, 85th ed. (CRC, Boca Raton, FL, 2004).

<sup>23</sup>I. Barin and O. Knacke, *Thermochemical Properties of Inorganic Substances* (Springer, Berlin, 1973).

<sup>24</sup>Y. Widjaja and C. B. Musgrave, *J. Chem. Phys.* **117**, 1931 (2002).

<sup>25</sup>Y. Widjaja and C. B. Musgrave, *Appl. Phys. Lett.* **80**, 3304 (2002).

<sup>26</sup>L. Jeloica, A. Estève, M. D. Rouhani, and D. Estève, *Appl. Phys. Lett.* **83**, 542 (2003).

<sup>27</sup>C. C. Surdu-Bob, S. O. Saied, and J. L. Sullivan, *Appl. Surf. Sci.* **183**, 126 (2001).

<sup>28</sup>T. Van Buuren, M. K. Weilmeier, I. Athwal, K. M. Colbow, J. A. Mackenzie, T. Tiedje, P. C. Wong, and K. A. R. Mitchell, *Appl. Phys. Lett.* **91**, 424 (1991).

<sup>29</sup>C. E. C. Wood, K. Singer, T. Ohashi, L. R. Dawson, and A. J. Noreika, *J. Appl. Phys.* **54**, 2732 (1983).

<sup>30</sup>G. D. Wilk and P. D. Ye (unpublished).